References

ALEXANDER, L. E. & SMITH, G. S. (1962). *Acta Cryst.* **15**, 983–1004.
BRAGG, W. L., JAMES, R. W. & BOSANQUET, C. H. (1921). *Phil. Mag.* **41**, 309.
DENNE, W. A. (1971*a*). *J. Appl. Cryst.* **4**, 400.
DENNE, W. A. (1971*b*). *J. Appl. Cryst.* **4**, 60–66.
DENNE, W. A. (1977*a*). *Acta Cryst.* A**33**, 438–440.
DENNE, W. A. (1977*b*). *J. Appl. Cryst.* To be published.
DENNE, W. A. (1977*c*). Unpublished.
DYSON, N. A. (1973). *X-rays in Atomic and Nuclear Physics*, pp. 83, 129, London: Longman.
FURNAS, T. C. JR (1965). *Trans. Amer. Cryst. Assoc.* **1**, 67–85.
HEITLER, W. (1957). *The Quantum Theory of Radiation*, pp. 181–188. Oxford Univ. Press.
LADELL, J., PARRISH, W. & TAYLOR, J. (1959). *Acta Cryst.* **12**, 561–570.
YOUNG, R. A. (1961). Tech. Rep. No. 2, Project No. A-389, Office of Naval Research, Washington 25, DC.

Acta Cryst. (1977). A**33**, 992–996

Short-Range Order to Long-Range Order Transition in Rare-Earth Metal Oxide Thin Crystals

BY V. K. KAUL AND U. SAXENA

Department of Physics, Banaras Hindu University, Varanasi-221005, *India*

(*Received* 28 *March* 1977; *accepted* 1 *June* 1977)

The rare-earth metal oxides are known to exhibit several phases which can be either stoichiometric or nonstoichiometric. One such phase which has been recently found to exist in thin-film form corresponds to the monoxide phase *RO*. The oxygen content in this phase, however, has been found to vary such that the phase actually has the stoichiometry RO_x with $1<x<2$. The present paper deals with electron diffraction studies of the SRO → LRO transition in the nonstoichiometric RO_x phase. This transition commences as a result of the creation of oxygen vacancies in the as-grown thin-film phase, when this phase is pulse annealed with an electron beam in the electron microscope, the annealing temperature being about 500 °C. The short-range ordered version is manifested by the appearance of curious diffuse streaks on the diffraction patterns. The diffuse intensity distribution has been found to be situated on a complicated surface (rhombic dodecahedron) in the reciprocal space of the initial f.c.c. phase with $a=5{\cdot}09\pm 0{\cdot}05$ Å and $5{\cdot}37\pm 0{\cdot}05$ Å for erbium and dysprosium oxides respectively. On further pulse annealing at a higher temperature (~900 °C), the short-range ordered version yields to give rise to a long-range ordered superlattice phase which corresponds to the bulk-like b.c.c. phase with $a=10{\cdot}41\pm 0{\cdot}05$ Å and $10{\cdot}18\pm 0{\cdot}05$ Å for erbium and dysprosium oxides respectively. The SRO → LRO transition has also been analysed in terms of the stoichiometric variations resulting from the pulse annealing.

Introduction

Solid-state materials with possible applications have aroused considerable attention, and a large amount of work has been done on them in the recent past. Rare-earth metal oxides form one such class of materials. These are materials capable of being used at high temperatures and have been found to possess interesting dielectric and semiconducting properties (Alper, 1970; Murr, 1967; Tsutsumi, 1970). These oxides, both in bulk and thin-film forms have been found to possess several structural phases (Murr, 1967; Eyring & Holmberg, 1963; Roth & Schneider, 1960; Eick, Baenzigner & Eyring, 1956; Bist, Kumar & Srivastava, 1972). These structural variants exhibit several stoichiometric variations, ranging from the simplicity of the R_2O_3 (R=rare earth metal) phase, whose crystallographic characterization is well established, through the monoxide phase *RO*, which is reasonably well understood, to the rather complicated nonstoichiometric variants, where much less is known in regard to both their existence and the structural details (Murr, 1967; Eick *et al.*, 1956; Bist *et al.*, 1972; Semiltov, Imamov, Ragimli & Man, 1976; Saxena & Srivastava, 1976, 1977; Kaul & Srivastava, 1976). Also, not much work is available relating to the solid-state transformations between one stoichiometric phase and another. Since the physical properties are phase dependent (Murr, 1967; Saxena & Srivastava, 1976), studies involving details of the stability and structural transformations are of obvious importance and need to be looked further into. The present paper deals with an interesting type of transformation in rare-earth metal oxide thin films, particularly those of erbium and dysprosium where the initial and the final phases exhibit long-range order (LRO), these phases being f.c.c. and b.c.c. respectively. The transformation, however, proceeds through an intermediate phase showing short-range order (SRO), which is displayed by the appearance of the diffuse intensity distribution on the diffraction patterns. In passing, it may be mentioned that this type of transformation has recently been reported in the case of In_2Te_3 and the chalcogenides of niobium and molybdenum (Bleris, Karakostas, Stoemensons &

Economou, 1976; Karakostas & Economou, 1975; Van Landuyt, Van Tendeloo & Amelinckx, 1974; Van Tendeloo, De Ridder & Amelinckx, 1975; Iijima, 1975; De Ridder, Van Tendeloo, Van Landuyt, Van Dyck & Amelinckx, 1976). Evidence and arguments have been advanced to show that SRO in the present case arises from the creation and ordering of oxygen vacancies. It has been found that the diffuse intensity is situated on a surface (rhombic dodecahedron) in the reciprocal space of the parent f.c.c. phase. The relevance of the SRO in the stabilization of LRO, which appears in the form of a superlattice based on the parent f.c.c. phase, has been studied and analysed.

Experimental

Thin films of erbium and dysprosium oxides were prepared by the vacuum evaporation of Er_2O_3 and Dy_2O_3 powder (99·9% pure) on copper supporting grids in a vacuum of about 10^{-6} torr. The films employed in the present investigations had thicknesses ranging between 500 and 700 Å. The films were examined in the electron microscope by employing both the imaging and the diffraction techniques. For the study of the phase transformations, the films were pulse annealed inside the electron microscope by taking out the condenser aperture for short periods (few minutes) and employing a precalibrated focused electron beam. The annealing temperatures obtained in such pulse annealing treatments were close to either 500 °C or 900 °C, depending upon the beam current employed. These temperatures were determined by noticing (*a*) the melting of antimony (melting point ~630 °C) and tellurium (~450 °C) films, (*b*) the occurrence of the α–γ transformation in iron foils (transformation temperature ~910 °C). In order that the changes in the diffraction patterns consequent to the pulse annealing treatment could be noted, the diffraction patterns were recorded before as well as after annealing. The recordings were made under the normal beam illumination condition and the temperature of the specimen presumably corresponds to a temperature which is very nearly the room temperature. In order to have unambiguous identification of the diffuse intensity distribution, the diffraction patterns were obtained with symmetrical excitation.

Results and discussion

Electron microscope studies of the oxide films prepared by the foregoing method revealed that the films were polycrystalline and the powder diffraction patterns from the initial phase corresponded to f.c.c. phase with lattice parameters 5·09 ± 0·05 and 5·37 ± 0·05 Å for erbium and dysprosium oxides respectively (Fig. 1). However, these lattice parameters were found to vary slightly from specimen to specimen, suggesting the possibility of non-stoichiometry in the oxide phase.

When the as-deposited f.c.c. phase was pulse annealed in the electron microscope, curious changes commenced in the diffraction patterns corresponding to the f.c.c. phase. The first noticeable change which ensued as a result of pulse annealing at about 500 °C was in regard to the appearance of diffuse streaks as well as the f.c.c. spots. Fig. 2 shows a single-crystal diffraction pattern in (111) orientation. It can easily be seen that, besides the six intense spots of 220 type (marked by *A*) from the parent f.c.c. phase, diffuse streaks also appear in the diffraction pattern. These streaks extend along ⟨110⟩ directions and often merge together to form triangular-shaped figures. Some of these triangles can be seen near the regions marked by *T* in Fig. 2. An interesting additional feature accompanying the diffuse streaks was the presence of a rather sharp spot (marked by arrow), located at the centroid of the triangle *T*. This spot and all equivalent ones in fact arise because of the intersection of ⟨111⟩ streaks with the Ewald sphere. This is evidenced by tilting experiments during which the intensities of other spots change, while, although these spots move, their intensity remains unchanged. We will later discuss the origin of these streaks. It should be mentioned that similar diffraction patterns were obtained for both erbium and dysprosium oxide specimens, and the representative figures which have been given can refer to any one of these.

Fig. 3 represents yet another diffraction pattern, in (110) orientation, in which the diffuse intensity is distinctly discernible. In this case the diffuse intensity lies on ellipses, some of which have been marked by *E* in Fig. 3. It can be noticed that the diffuse intensity is not quite uniform around the ellipse. In particular, it is negligibly small at the ends of the minor axes and large near the ends of the major axes. Fig. 4 represents yet another reciprocal lattice projection, (211). In this case the diffuse intensity lies along a ⟨111⟩ direction. The sharp spot in the centre, which has been marked with an arrow is again the result of the intersection of ⟨111⟩ streaks with the Ewald sphere.

The origin and location of diffuse intensity distribution

As is well known, the diffuse intensity may arise from (i) thermal vibrations of atoms, (ii) size effects and Huang scattering, and (iii) short-range ordering of atoms and vacancies.

Since all the diffraction patterns exhibiting the diffuse intensity were taken with the specimen under normal beam illumination, *i.e.* with the specimen nearly at room temperature, the diffuse intensity cannot have a thermal origin. The sizes of the metal and oxygen atoms are not very different. This fact, coupled with the observation that the diffuse intensity is not confined to near the fundamental Bragg reflexions but extends along lines or curves, and disappears on repeated pulse annealing at higher temperatures (~900 °C), rules out the size effects and Huang scattering as being responsible for the occurrence of the diffuse intensity. Thus it seems that short-range ordering

is the most likely reason for the appearance of the diffuse intensity. Further evidence and arguments in support of this are given in the following.

The rare-earth metal oxides are known to possess nonstoichiometry in regard to their oxygen content, (Bist *et al.*, 1972; Semiltov *et al.*, 1976; Kaul & Srivastava, 1976; Saxena & Srivastava, 1977; Error & Wagner, 1968). Both the present authors and Semiltov and his coworkers have obtained evidence for the presence of this nonstoichiometry in thin films of rare-earth metal oxides (Bist *et al.*, 1972; Semiltov *et al.*, 1976; Kaul & Srivastava, 1976; Saxena & Srivastava, 1977). These films have been found to have a stoichiometry different from that of the bulk phase, which is b.c.c. and has the stoichiometry corresponding to $RO_{1\cdot5}$. The thin-film phase, which is f.c.c., has been referred to as a monoxide phase with the oxygen content often varying from the exact monoxide RO stoichiometry. Precise Fourier analysis based on diffraction patterns of the oxide thin films has revealed that the oxygen content in these oxide films may be large, and therefore, although the oxides are f.c.c., they are not quite like RO, which has ZnS-type structure, but are RO_x type with $1 < x < 2$ and tend to have a structure approaching that of CaF_2. This implies that the oxygen content in thin films is higher than in the bulk phase. This, however, is expected in the light of the fact that the starting material for the preparation of thin films was $RO_{1\cdot5}$ and thermal evaporation may lead to the incorporation of additional oxygen leading to the formation of RO_x ($x > 1\cdot5$).

Now pulse annealing treatment of transition metal oxides, including rare-earth metals, in the electron microscope is known to produce loss of oxygen and thus results in the creation of oxygen vacancies (Bursill, 1969; Bist *et al.*, 1972; Seltzer & Zafee, 1973; Iijima, 1975). Although the mechanism of the reduction is not known, it is thought that the increase of the temperature of the specimen coupled with the energy transfer from the electron beam may be responsible for this reduction (Iijima, 1975). It has also been conjectured that the contamination of the specimen in the electron microscope may initiate catalytic reactions leading to oxygen loss (Iijima, 1975). Even though the exact mechanism of reduction is not known, several nonstoichiometric oxide phases with oxygen deficiency have been produced through electron-beam pulse annealing (Bursill, 1969; Bist *et al.*, 1972; Seltzer & Zafee, 1973; Iijima, 1975). Thus in the present case, the pulse annealing treatment of oxide films may be taken to result in the oxygen loss in the oxide samples. This would apparently produce oxygen vacancies on the oxygen sublattice and would represent a binary system which can undergo disorder–order transitions. The diffuse intensity would thus correspond to the short-range ordering of oxygen vacancies on the oxygen sublattice. However, the sharpness of the diffuse streaks on the diffraction patterns (see Figs. 2 and 3) reveals that the SRO observed here is somewhat different from that usually observed in binary alloys. In the present case SRO contains ordering correlation up to 100 Å.

In order to deduce the location of the diffuse intensity in the reciprocal space, diffraction patterns in several orientations were examined, and tilting experiments were carried out to obtain additional information. The following are the salient points regarding the intensity distribution in reciprocal space:

(*a*) The low-index reciprocal-lattice orientations revealed the presence of diffuse intensity along simple lines or curves. For example, in (111) orientation, the diffuse intensity was confined along lines parallel to ⟨110⟩ directions (see Fig. 2) whereas in (110) orientation, it was confined around ellipses (see Fig. 3). In (100) orientation, no significant diffuse intensity was observed.

(*b*) As the thin single crystal regions exhibiting the low-index reciprocal projections were tilted through a few degrees, the diffuse intensity distribution became much more pronounced but more complicated. This is clearly seen in Fig. 5, which represents the diffraction pattern corresponding to a (111) tilted orientation. Similar features were also observed for other tilted low-index orientations. The foregoing feature brings out an important fact regarding the location of the diffuse intensity. There is much more diffuse intensity distributed on high-index reciprocal lattice planes than on the low-index ones.

These observations suggested that the diffuse intensity was distributed over some sort of surface in reciprocal space, most of the positions of which were not contained in the low-index reciprocal-lattice planes. It is opportune to mention here that recently the location of diffuse intensity on surfaces has been reported in the case of nonstoichiometry-induced SRO in several other materials such as In_2Te_3, VC, TiO (Bleris *et al.*, 1976; Karakostas & Economou, 1975; Sauvage & Parthé, 1972; Billingham, Bell & Lewis, 1972; Castles, Cowley & Spargo, 1971).

With the above features kept in mind, several surfaces were tried. It was found that the best match was obtained when the diffuse intensity was taken to be situated on a rhombic dodecahedron in the b.c.c. reciprocal unit cell of the original f.c.c. phase. This is shown in Fig. 6. The match between expected and observed diffuse intensities is brought out in Figs. 7 and 8. It may be seen that the triangular arrangement of diffuse streaks in (111) section and the nearly elliptical arrangement in (110) section are clearly brought out in these figures. It may also be noticed that for the (110) section, there are portions near the vertices of the ellipse which are directly contained in the plane section. Thus, these will lie almost exactly on the Ewald sphere (which will be nearly planar), whereas the portions off the plane, marked by crosses in Fig. 3, would be away from the Ewald sphere, and thus would come out rather faint.

As regards the appearance of the points at the centroid of the diffuse intensity triangle (Fig. 2), these ap-

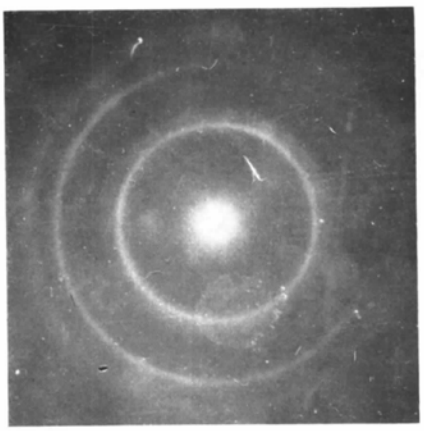

Fig. 1. Powder diffraction pattern from a polycrystalline as-grown film of dysprosium oxide exhibiting the initial f.c.c. phase ($a = 5.37 + 0.05$ Å).

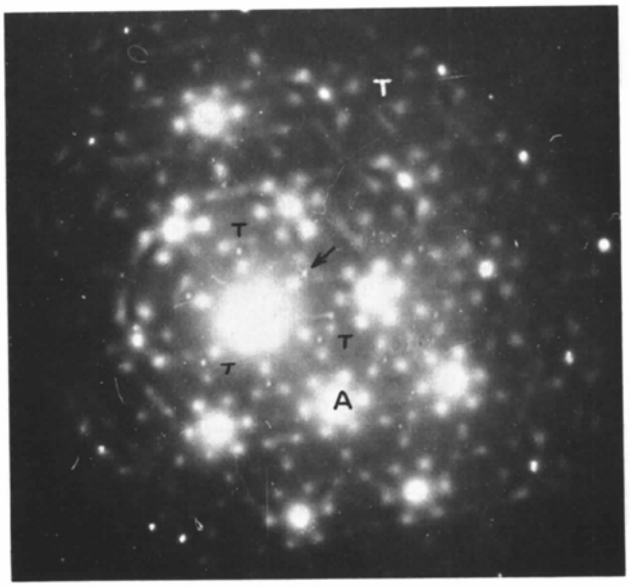

Fig. 2. (111) section of the single-crystal diffraction pattern from the erbium oxide film. Notice the appearance of diffuse streaks which often cluster to form triangle-shaped figures (some of them are marked by *T*). The presence of a spot marked by an arrow at the centroid of the triangle *T* can also be noted. This spot (and other equivalent ones) arise from ⟨111⟩ direction streaks. The spots marked by *A* correspond to 220-type reflexions from the initial f.c.c. phase.

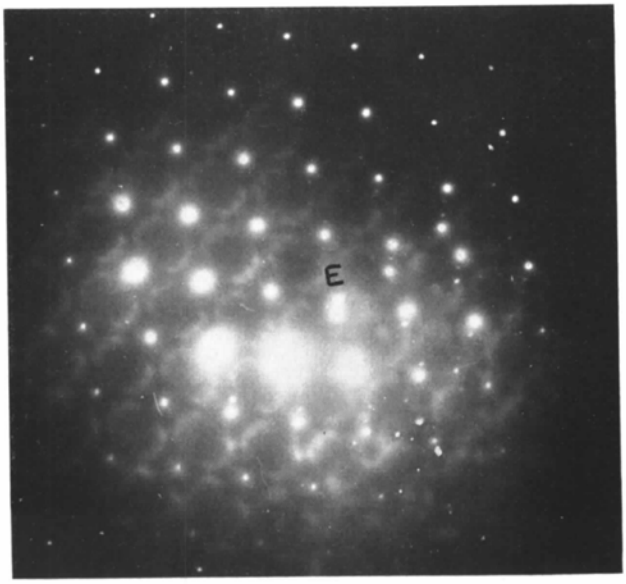

Fig. 3. (110) section of the single-crystal diffraction pattern from the dysprosium oxide film. The diffuse streak in this case lies around an ellipse, as shown by *E*.

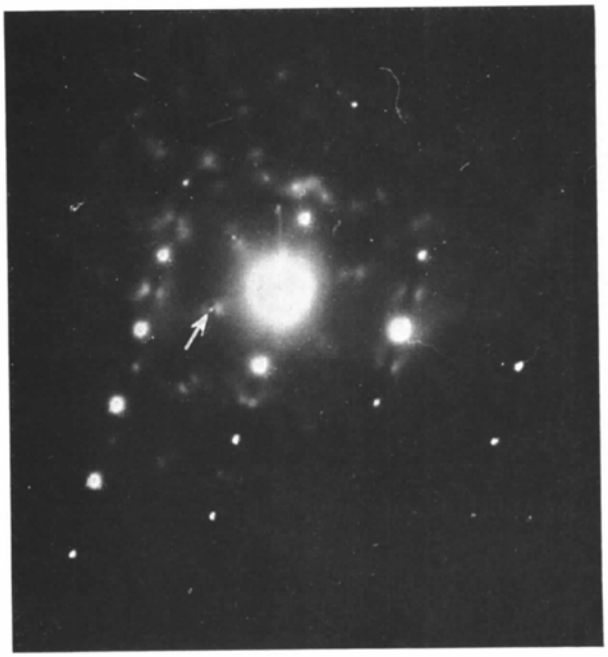

Fig. 4. (211) section of the single-crystal diffraction pattern from the dysprosium oxide film. Notice the presence of a spot marked by an arrow.

[*To face p.* 994

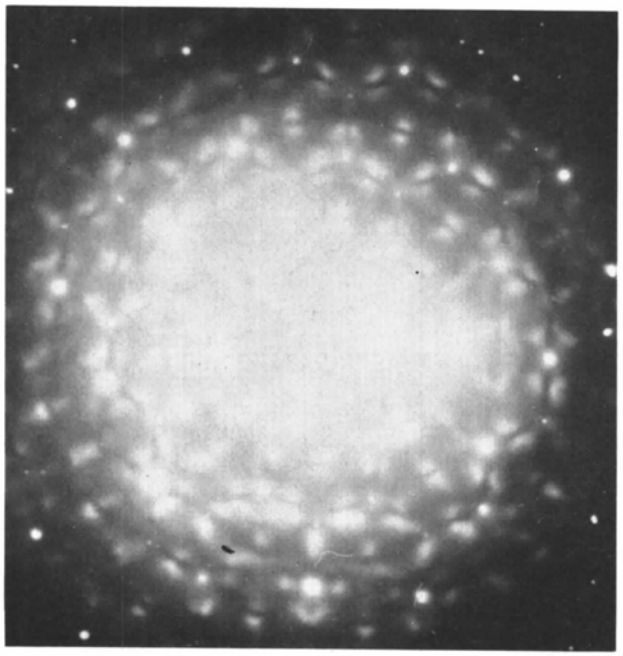

Fig. 5. Single-crystal diffraction pattern of dysprosium oxide film corresponding to an orientation which is somewhat tilted with respect to (111).

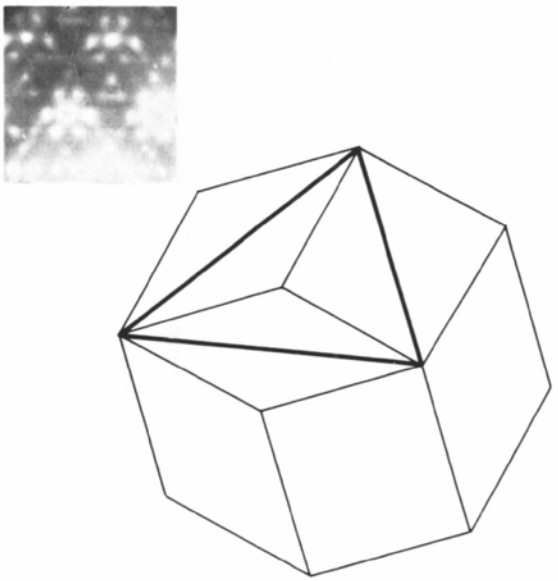

Fig. 7. (111) section through the rhombic dodecahedron. Notice the triangular-shaped intersection (shown by thick lines) representing the observed diffuse intensity distribution in this orientation.

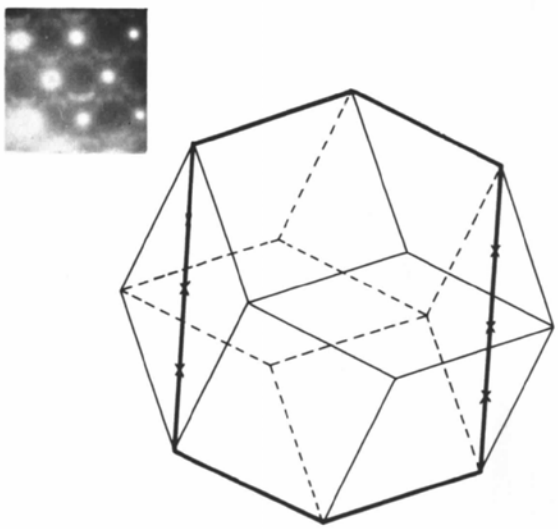

Fig. 8. (110) section through the rhombic dodecahedron. In this case the intersection is nearly elliptical and resembles closely the observed diffuse intensity distribution for this orientation. The crossed regions of the ellipse represent the regions where the diffuse intensity distribution is expected to be very feeble.

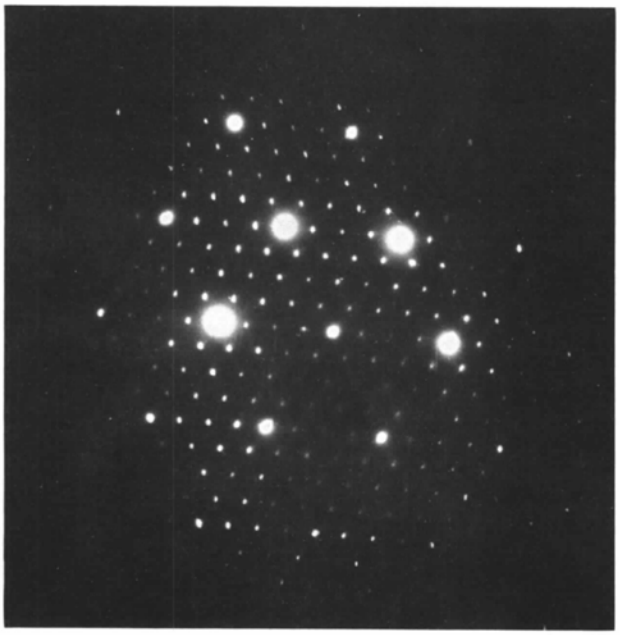

Fig. 9. Single-crystal diffraction pattern in (111) orientation for the erbium oxide film. This pattern exhibits the LRO superlattice phase. Notice that, instead of streaks, sharp spots appear which represent the ordered phase.

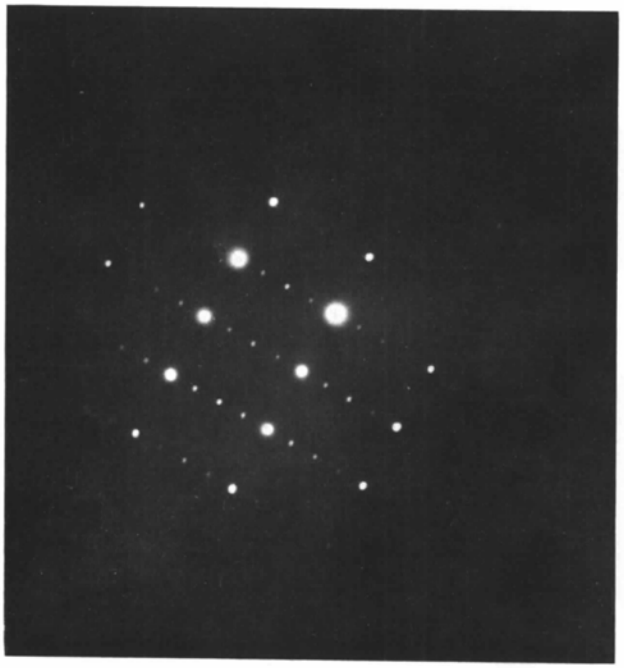

Fig. 10. Single-crystal diffraction pattern of the LRO phase in (211) orientation for erbium oxide film.

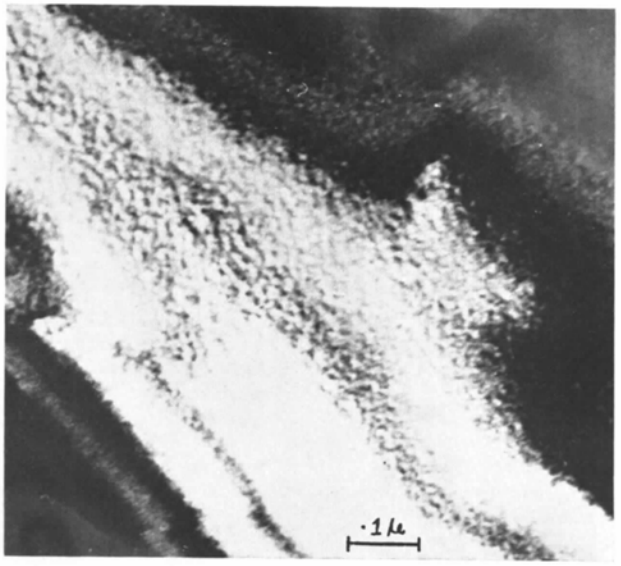

Fig. 11. Dark-field micrograph of dysprosium oxide film taken by employing the diffuse streak. The presence of micro-domains can be easily seen.

parently arise as a result of disorder, which virtually amounts to displacement of (111) lattice planes. If the oxygen vacancies which are created during the pulse annealing cluster to form rows along the ⟨110⟩ direction on the {111} planes and if these rows do not coincide for the various {111} planes, a diffuse intensity spike parallel to a ⟨111⟩ direction will result in reciprocal space. The sharpness of the spot suggests that these displacements amongst the {111} planes are significantly large. It should be mentioned that clustering and the resulting correlation in oxygen vacancies are expected along ⟨110⟩ directions, this being the direction of the close packing (Billingham *et al.*, 1972). This effect would be important for the SRO streaks as well as for the ⟨111⟩ direction streaks.

When the SRO phase was repeatedly pulse annealed at higher temperatures (~900 °C) and the specimens exhibiting this phase were re-examined under normal beam illumination, it was found that the diffuse streaks and therefore the SRO had disappeared. A superlattice manifested by the appearance of sharp spots was found at nearly the same positions as the diffuse streaks. The correlation between the positions of the diffuse streaks and resulting sharp spots suggested that the SRO had yielded to LRO. The representative diffraction patterns exhibiting this LRO are shown in Figs. 9 and 10. It was found that this LRO superlattice actually corresponds to the b.c.c. phase with lattice parameter very nearly the same as that of the bulk phase. Intensities of the diffraction spots of the LRO phase were found to be in good agreement with those expected from the bulk-type phase. The superlattice b.c.c. has $a = 10{\cdot}41 \pm 0{\cdot}05$ and $a = 10{\cdot}18 \pm 0{\cdot}05$ Å for erbium and dysprosium oxides respectively, the corresponding parameters for the bulk phases being $a = 10{\cdot}55$ and $a = 10{\cdot}665$ Å. The appearance of this LRO phase, which is nearly the same as the bulk phase, can be explained in terms of stoichiometric variations resulting from oxygen loss on pulse annealing. As mentioned previously, the as-prepared samples may be taken to have excess of oxygen corresponding to formula RO_x with $x > 1{\cdot}5$. It should be pointed out that, whereas the phase corresponding to RO is known to be f.c.c. with ZnS-type structure, the other phases having RO_x with $x > 1$ are still f.c.c. but tend towards the CaF_2-type structure. The phase RO_x with $x = 2$ actually corresponds to CaF_2-type structure. If the as-prepared film has $x > 1{\cdot}5$, the pulse annealing will lead to the loss of oxygen and when the oxygen content is such that $x = 1{\cdot}5$, it would result in the formation of a b.c.c. phase which is nearly the same as the bulk phase. It should be mentioned that the b.c.c. phase is a deficient CaF_2-type structure where only $\frac{3}{4}$ of the oxygen atoms are present. Because of this deficiency in oxygen the metal sublattice is distorted and the resulting structure is complicated (Wyckoff, 1964); however, the b.c.c. LRO phase can still be looked upon as having an approximate CaF_2-type structure. The pulse-annealing treatment presumably produces some correlation in the atom-vacancy positions on the oxygen sublattice, giving rise to the existence of SRO. The absence of either SRO or LRO in the initial as-grown film suggests that the pulse annealing is responsible for the production and ordering of the oxygen vacancies. It should be pointed out that the $RO_{1{\cdot}5}$ (R_2O_3) represents the most stable stoichiometric phase in the rare-earth metal oxides. Therefore, once the oxygen loss produces the stoichiometry corresponding to the stable phase, further reduction is not expected to take place. This has actually been found, since in the present observation as well as in other similar observations (Murr, 1967), the R_2O_3-type oxide thin-film phase does not undergo any further reduction on further pulse annealing. The b.c.c.-type R_2O_3 phase as formed in the present investigation through SRO → LRO transformation has a slightly different lattice parameter from that of the corresponding bulk phase. This may be because the LRO phase still has some excess or deficiency of oxygen, but with the corresponding oxygen atom or vacancy positions having very feeble or no correlation.

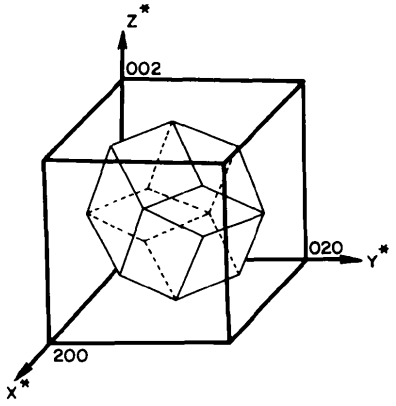

Fig. 6. The rhombic dodecahedron representing the diffuse intensity distribution. The dodecahedron has been shown with respect to the b.c.c. reciprocal unit cell.

The crystallographic characterization of the SRO state may be carried out in terms of either of two models (Karakostas & Economou, 1975; Bleris *et al.*, 1976; Sauvage & Parthé, 1972; Billingham *et al.*, 1972): (1) the statistical model embodying the non-random atom-pair probabilities and (2) the 'microdomain' model in which discrete regions having long-range atom correlations are dispersed in a matrix which is disordered. To distinguish between the two possibilities dark-field micrographs were taken. These pictures reveal the presence of 'microdomains'. A representative example is given in Fig. 11. As regards the polyhedral clusters representing the SRO and giving the observed type of diffuse intensity distribution, it was found that in the present case it was not possible to work out any simple type of polyhedron which is capable of representing correctly all the observed features of the diffuse intensity distribution (De Ridder, Van Tendeloo & Amelinckx, 1976). It may be possible that the type of

the diffuse intensity observed in the present case would involve several types of polyhedra with varying stoichiometry, as in the case of In_2Te_3 (Karakostas & Economou, 1975; Bleris *et al.*, 1976). However, since the main emphasis of the present work was not the working out of the cluster models, rigorous attempts were not made to work out the details of the microscopic polyhedral clusters representing the diffuse intensity distribution.

In summary it can be said that the rare-earth metal oxide film specimens undergo a SRO → LRO transition. The transition occurs by the creation and ordering of oxygen vacancies as a result of pulse annealing the as-grown thin oxide films. A curious diffuse intensity distribution represents the SRO state and the analysis of this distribution reveals that it is located on a rhombic dodecahedron in the reciprocal space of the initial f.c.c. phase. Pulse annealing at higher temperatures ($\sim$900 °C) initiates the SRO → LRO transition which is marked by the disappearance of the diffuse streaks and the appearance of an ordered superlattice phase. This phase is very much akin to the bulk phase. Although the present investigation has been concerned with erbium and dysprosium oxides, preliminary investigations reveal that similar transformations also occur for other rare-earth metal oxide film specimens.

The authors are grateful to Dr O. N. Srivastava of this department for suggesting the present work. They thank Professor A. Guinier for extensive discussions during his stay as Visiting Professor in December 1976. The authors are also grateful to Dr G. Van Tendeloo for helpful discussions and to CSIR for the award of the Senior Research Fellowship.

References

ALPER, A. M. (1970). *High Temperature Oxides.* Part II. *Oxides of Rare Earths, Titanium, Zirconium, Hafnium, Niobium and Tantalum.* pp. 42–59. New York: Academic Press.

BILLINGHAM, J., BELL, P. S. & LEWIS, M. H. (1972). *Acta Cryst.* A**28**, 602–606.

BIST, B. M. S., KUMAR, J. & SRIVASTAVA, O. N. (1972). *Phys. Stat. Sol.* (*a*), **14**, 197–206.

BLERIS, G. L., KARAKOSTAS, T., STOEMENSONS, J. & ECONOMOU, N. A. (1976). *Phys. Stat. Sol.* (*a*), **34**, 243–254.

BURSILL, L. A. (1969). *Proc. Roy. Soc.* A**311**, 267–290.

CASTLES, J. R., COWLEY, J. M. & SPARGO, A. E. C. (1971). *Acta Cryst.* A**27**, 376–383.

DE RIDDER, R., VAN TENDELOO, G. & AMELINCKX, S. (1976). *Acta Cryst.* A**32**, 216–224.

DE RIDDER, R., VAN TENDELOO, G., VAN LANDUYT, J., VAN DYCK, D. & AMELINCKX, S. (1976). *Phys. Stat. Sol.* (*a*), **37**, 591–606.

EICK, H. A., BAENZIGNER, N. C. & EYRING, L. (1956). *J. Amer. Chem. Soc.* **78**, 5147–5150.

ERROR, N. G. & WAGNER, J. B. JR (1968). *J. Phys. Chem. Solids*, **29**, 1597–1611.

EYRING, L. & HOLMBERG, B. (1963). *Advanc. Chem. Ser.* **39**, 46.

IIJIMA, S. (1975). *Acta Cryst.* A**31**, 784–790.

KARAKOSTAS, T. & ECONOMOU, N. A. (1975). *Phys. Stat. Sol.* (*a*), **31**, 89–99.

KAUL, V. K. & SRIVASTAVA, O. N. (1976). *Jap. J. Appl. Phys.* **15**, 1801–1802.

MURR, L. E. (1967). *Phys. Stat. Sol.* (*a*), **24**, 135–148.

ROTH, R. S. & SCHNEIDER, S. J. (1960). *J. Res. Natl. Bur. Stand.* **64A**, 300.

SAXENA, U. & SRIVASTAVA, O. N. (1976). *Thin Solid Films*, **33**, 185–192.

SAXENA, U. & SRIVASTAVA, O. N. (1977). *Thin Solid Films.* **42**, L2–4.

SAUVAGE, M. & PARTHÉ, E. (1972). *Acta Cryst.* A**28**, 607–616.

SELTZER, M. S. & ZAFEE, R. I. (1973). *Defects and Transport in Oxides*, pp. 177–203. New York: Plenum Press.

SEMILTOV, S. A., IMAMOV, R. A., RAGIMLI, N. A. & MAN, L. I. (1976). *Thin Solid Films*, **32**, 325–328.

TSUTSUMI, T. (1970). *Jap. J. Appl. Phys.* **9**, 735–739; *Toshiba Rev.*, March–April, 52–55.

VAN LANDUYT, J., VAN TENDELOO, G. & AMELINCKX, S. (1974). *Phys. Stat. Sol.* (*a*), **26**, 359–376.

VAN TENDELOO, G., DE RIDDER, R. & AMELINCKX, S. (1975). *Phys. Stat. Sol.* (*a*), **27**, 457–468.

WYCKOFF, R. W. G. (1964). *Crystal Structures*, 2nd ed., Vol. 2. New York: John Wiley.